Electronic Supplementary Material (ESI) for Journal of Materials Chemistry A.

Theoretical study on stability and ion transport property with halide doping of Na_3SbS_4 electrolyte for all-solid-state battery

Randy Jalem[a,b,c,*], Bo Gao,[a] Hong-Kang Tian,[a] and Yoshitaka Tateyama[a,c,*]

[a]Center for Green Research on Energy and Environmental Materials (GREEN), National Institute for Materials Science (NIMS), Tsukuba, Japan. E-mail: JALEM.Randy@nims.go.jp; Tel: +81-029-8604636 (ex. 4636).

[b]PRESTO, Japan Science and Technology Agency (JST), Saitama, Japan.

[c]Elements Strategy Initiative for Catalysts & Batteries, Kyoto University, Kyoto, Japan.

Table S1. Comparison of DFT lattice parameters with tetragonal Na_3SbS_4 as the initial structure for undoped and doped models.

Composition	**Initial structure**	**a_1 / Å**	**a_2 / Å**	**a_3 / Å**	**a_3/a_1**	**a_3/a_2**
Na_3SbS_4	Tetragonal (unit cell)	7.2207	7.2207	7.3729	1.0211	1.0211
$Na_{2.8750}SbS_{3.8750}Cl_{0.1250}$	Tetragonal (2x2x2)	7.2430	7.2574	7.3682	1.0173	1.0153
$Na_{2.9375}SbS_{3.9375}Cl_{0.0625}$*	-	7.176	7.176	7.183	1.0001	1.0001

*Experimental data (F. Tsuji et al., J. Ceram. Soc. Jpn 2020, 128, 641-647).

Table S2. Comparison between DFT results (in this work) and experiment (in parenthesis, based from Ref. 33 of main text) for the structural information of t-Na_3SbS_4.

Atom pair	**Bond distance / Å**	**%diff.**
Na1-S(1)	2.91 (2.87)	1.3
Na1-S(2)	2.91 (2.87)	1.3
Na1-S(3)	3.04 (3.02)	0.7
Na1-S(4)	3.04 (3.02)	0.7
Na1-S(5)	3.10 (3.06)	1.3
Na1-S(6)	3.10 (3.06)	1.3
Na2-S(1)	3.04 (3.01)	1.3
Na2-S(2)	3.04 (3.01)	1.3
Na2-S(3)	3.04 (3.01)	1.3
Na2-S(4)	3.04 (3.01)	1.3
Na2-S(5)	3.45 (3.42)	0.8
Na2-S(6)	3.45 (3.42)	0.8
Sb-S	2.36 (2.31)	2.3

Table S3. Variation of DFT-calculated lattice constants with halide anion doping on c-Na_3SbS_4.

DFT Composition	**Ave. lattice constant / Å (GGA-PBE @0 K)**	**%diff. (undoped vs. doped)**
c-Na_3SbS_4 (cubic)	7.2466	-
$Na_{2.875}SbS_{3.875}F_{0.125}$	7.2775	0.43
$Na_{2.875}SbS_{3.875}Cl_{0.125}$	7.2900	0.60
$Na_{2.875}SbS_{3.875}Br_{0.125}$	7.2887	0.58
$Na_{2.875}SbS_{3.875}I_{0.125}$	7.3100	0.87

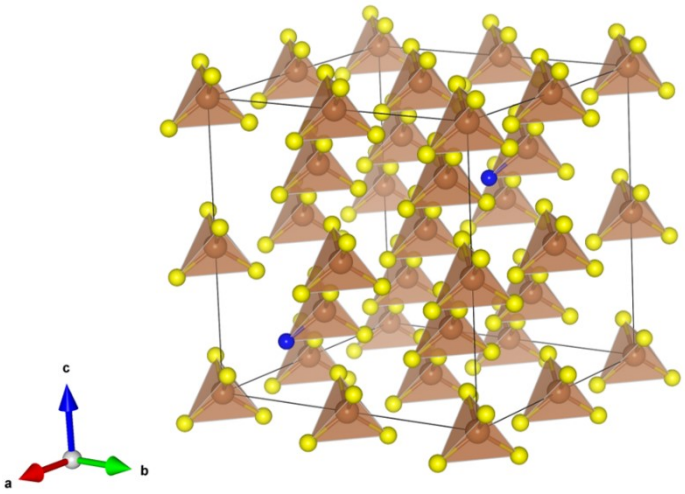

Figure S1. Schematic illustration of 2 x 2 x 2 c- Na_3SbS_4 supercell model showing the SbS_4 tetrahedral units (brown) and 2 S sites substituted by halide dopant atoms (blue).

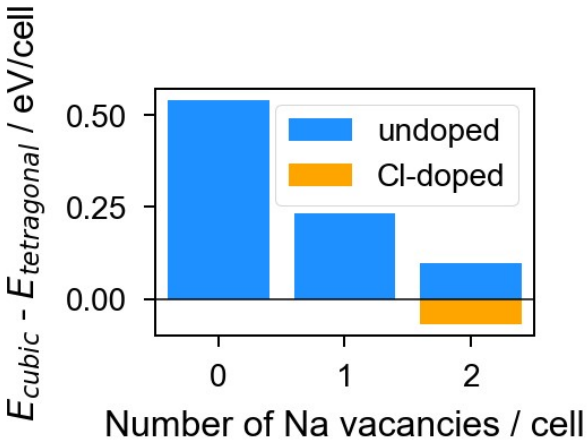

Figure S2. DFT energy difference between cubic and tetragonal structure as a function of number of vacancies. At each cell with a given number of Na vacancies (i.e., 1, and 2), a structure configuration sampling was performed followed by DFT geometry optimization (10 undoped tetragonal structures, 10 undoped cubic structures, 5 Cl-doped tetragonal structures, and 5 Cl-doped cubic structures). The lowest-energy structures for each cases were taken for the calculation of the energy difference between the cubic and tetragonal structure (i.e., $E_{cubic} - E_{tetragonal}$ / eV/cell).

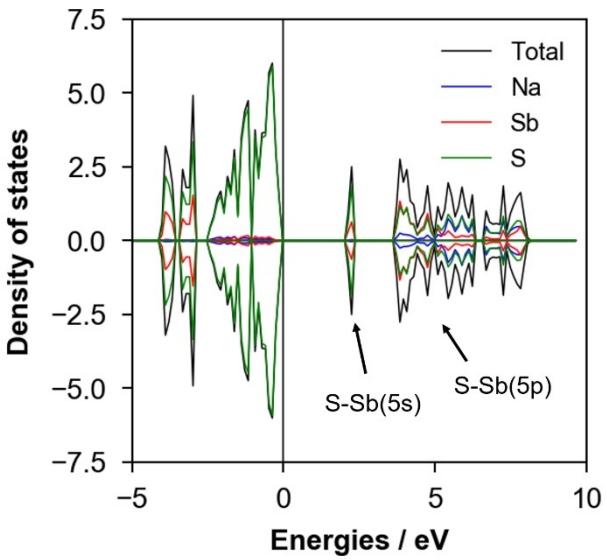

Figure S3. DFT-calculated total and partial density of states (DOS) of t-Na_3SbS_4 ($P42_1c$).

Table S4. Various phases in the Na-Sb-S system and their DFT-calculated formation energy (E_f). First entry (in bold letters) is for t-Na_3SbS_4 (cell composition: $Na_6Sb_2S_8$).

Cell composition			E_f / eV/atom	Cell composition			E_f / eV/atom	Cell composition			Ef / eV/atom
Na6	**Sb2**	**S8**	**-1.09905**	Na8			0.010761			S56	0.038013
Na12	Sb4	S12	-1.15974	Na4			0.003017			S32	0.04484
Na2	S4	Sb2	-1.01534	Na3			0.000231			S88	0.028838
Na3	S4	Sb1	-1.09459	Na2			0			S20	0.032116
Na2	Sb2	S4	-0.99488	Na8			0.069048			S28	0.020189
Na8	Sb8		-0.32833	Na1			0.000106			S36	0.016808
Na6	Sb2		-0.43777	Na1			0.002694			S28	0.041008
Na4		S2	-1.19118	Na1			1.072084			S48	0.001343
Na8		S4	-1.25482		Sb2		0.280245			S24	0.015913
Na2		S1	-1.29437		Sb2		0.065751			S80	0.014414
Na6		S6	-1.16219		Sb1		0.324607			S104	0.028873
Na1		S1	-0.79163		Sb4		0.261254			S72	0.020778
Na4		S4	-1.16472		Sb4		0.114852			S72	0.037362
Na1		S1	-0.66411		Sb1		0.311715			S18	0.355
	Sb8	S12	-0.65163		Sb1		0.234278			S4	1.122607
	Sb8	S20	-0.43184		Sb1		0.048567			S4	0.342059
	Sb17	S27	-0.58276		Sb2		0			S4	0.343461
	Sb11	S18	-0.56467		Sb14		0.315406			S6	0.06543
	Sb2	S4	-0.31157			S32	0			S1	0.621523
	Sb2	S2	-0.36271			S32	0.000961			S4	0.509846
Na4			0.128501			S18	0.442006			S9	0.04123
Na1			0.0026			S8	0.010616			S1	1.298147

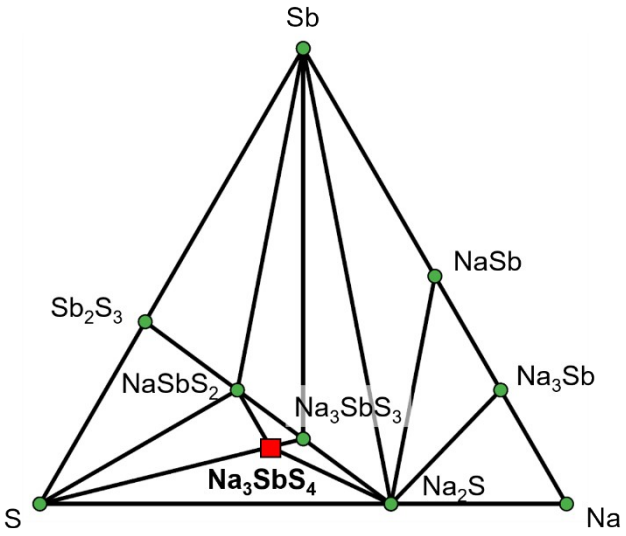

Figure S4. Na-Sb-S thermodynamic phase diagram. Na_3SbS_4 is indicated by a red square.

Table S5. Detailed chemical reactions and critical chemical potentials from grand potential phase diagram analysis for open transition metal (TM) species for different layered-type Na[TM]O_2 (TM = {V, Cr, Mn, Fe, Co, Ni}) cathode compounds. Note: $\mu_V = 0$, $\mu_{Cr} = 0$, $\mu_{Mn} = 0$, $\mu_{Fe} = 0$, $\mu_{Co} = 0$, and $\mu_{Ni} = 0$ are referenced to the chemical potentials of V metal (μ_V^0= -9.0866 eV), Cr metal (μ_{Cr}^0 = -9.6367 eV), Mn metal (μ_{Mn}^0 = -9.1592 eV), Fe metal (μ_{Fe}^0 = -8.4598 eV), Co metal (μ_{Co}^0 = -7.1100 eV), and Ni metal (μ_{Ni}^0 = -5.7811 eV), respectively.

Compound	**Open TM element**	**Critical reactions (μ_{TM} relative to μ_{TM}^0)**
$NaVO_2$ (@full sodiation)	V	$NaVO_2$ → $NaVO_2$ (0 eV) $NaVO_2$ → 0.2222 V_2O_3 + 0.3333 Na_3VO_4 + 0.2222 V (-1.7950 eV)
VO_2 (@full desodiation)	V	2 VO_2 → 2 VO_2 (-3.071 eV) 2 VO_2 → 0.5714 V_3O_7 + 0.2857 V (-4.7314 eV)
$NaCrO_2$ (@full sodiation)	Cr	$NaCrO_2$ → $NaCrO_2$ (0 eV) $NaCrO_2$ → 0.5 Na_2CrO_4 + 0.5 Cr (-4.0055 eV)
CrO_2 (@full desodiation)	Cr	2 CrO_2 → 2 CrO_2 (-4.9986 eV) 2 CrO_2 → 0.3333 Cr_5O_{12} + 0.3333 Cr (-5.5896 eV)
$NaMnO_2$ (@full sodiation)	Mn	2 $NaMnO_2$ → 2 $NaMnO_2$ (-0.2598 eV) 2 $NaMnO_2$ → 0.75 Na_2MnO_3 + 0.25 $Na_2Mn_3O_7$ + 0.5 Mn (-3.5522 eV)
MnO_2 (@full desodiation)	Mn	4 MnO_2 → 4 MnO_2 (-3.9869 eV) 4 MnO_2 → 4 O_2 + 4 Mn (-5.4311 eV)
$NaFeO_2$ (@full sodiation)	Fe	2 $NaFeO_2$ → 2 $NaFeO_2$ (0 eV) 2 $NaFeO_2$ → 2 NaO_2 + 2 Fe (-5.0297 eV)
FeO_2 (@full desodiation)	Fe	2 FeO_2 + 0.6667 Fe → 1.333 Fe_2O_3 (-0.9179 eV) 2 FeO_2 → 2 O_2 + 2 Fe (-4.7154 eV)
$NaCoO_2$ (@full sodiation)	Co	2 $NaCoO_2$ → 2 $NaCoO_2$ (-0.0769 eV) 2 $NaCoO_2$ → 0.4 $Na_3(CoO_2)_4$ + 0.2 Na_4CoO_4 + 0.2 Co (-2.7802 eV)
CoO_2 (@full desodiation)	Co	4 CoO_2 → 4 CoO_2 (-3.0933 eV) 4 CoO_2 → 4 O_2 + 4 Co (-3.4132 eV)
$NaNiO_2$ (@full sodiation)	Ni	2 $NaNiO_2$ → 2 $NaNiO_2$ (-0.3627 eV) 2 $NaNiO_2$ → 2 NaO_2 + 2 Ni (-2.1525 eV)
NiO_2 (@full desodiation)	Ni	NiO_2 + 0.5 Ni → 0.5 Ni_3O_4 (-1.7025 eV) NiO_2 → O_2 + Ni (-1.9185 eV)

Table S6. Detailed chemical reactions and critical chemical potentials from grand potential phase diagram analysis for open transition metal (TM) species for different electrolyte/electrolyte-related compounds. Note: $\mu_V = 0$, $\mu_{Cr} = 0$, $\mu_{Mn} = 0$, $\mu_{Fe} = 0$, $\mu_{Co} = 0$, and $\mu_{Ni} = 0$ are referenced to the chemical potentials of V metal (μ_V^0= -9.0866 eV), Cr metal (μ_{Cr}^0 = -9.6367 eV), Mn metal (μ_{Mn}^0 = -9.1592 eV), Fe metal (μ_{Fe}^0 = -8.4598 eV), Co metal (μ_{Co}^0 = -7.1100 eV), and Ni metal (μ_{Ni}^0 = -5.7811 eV), respectively.

Compound	**Open TM element**	**Critical reactions (μ_{TM} relative to μ_{TM}^0)**
Na_3SbS_4	V	2 Na_3SbS_4 + 0.8 V → 0.8 Na_3SbS_3 + 1.2 $NaSbS_2$ + 0.8 Na_3VS_4 (-1.5665 eV) 2 Na_3SbS_4 → 2 Na_3SbS_4 (-3.2691 eV)
	Cr	2 Na_3SbS_4 + 1.333 Cr → 1.333 $NaCrS_2$ + 0.6667 $NaSbS_2$ + 1.333 Na_3SbS_3 (-1.0402 eV) 2 Na_3SbS_4 → 2 Na_3SbS_4 (-2.0617 eV)
	Mn	2 Na_3SbS_4 + Mn → 2 Na_3SbS_3 + MnS_2 (-0.8262 eV) 2 Na_3SbS_4 → 2 Na_3SbS_4 (-1.6204 eV)
	Fe	2 Na_3SbS_4 + Fe → 2 Na_3SbS_3 + FeS_2 (-0.5356 eV) 2 Na_3SbS_4 → 2 Na_3SbS_4 (-1.4968 eV)
	Co	2 Na_3SbS_4 + Co → CoS_2 + 2 Na_3SbS_3 (-0.9348 eV) 2 Na_3SbS_4 → 2 Na_3SbS_4 (-1.0114 eV)
	Ni	2 Na_3SbS_4 + 1.5 Ni → 2 Na_3SbS_3 + 0.5 Ni_3S_4 (-0.4050 eV) 2 Na_3SbS_4 → 2 Na_3SbS_4 (-0.8448 eV)
Na_3SbS_3	V	4 Na_3SbS_3 + 2.4 V → 2.4 Na_3VS_4 + 2.4 Na_2S + 4 Sb (-1.0179 eV) 4 Na_3SbS_3 → 4 Na_3SbS_3 (-1.3927 eV)
	Cr	4 Na_3SbS_3 + 4 Cr → 4 $NaCrS_2$ + 4 Na_2S + 4 Sb (0 eV) 4 Na_3SbS_3 → 4 Na_3SbS_3 (-0.8664 eV)
	Mn	4 Na_3SbS_3 + 6 Mn → 2 Na_6MnS_4 + 4 MnS + 4 Sb (-0.0674 eV) 4 Na_3SbS_3 → 4 Na_3SbS_3 (-0.4704 eV)
	Fe	4 Na_3SbS_3 + 6 Fe → 2 FeS + 4 FeSbS + 6 Na_2S (0 eV) 4 Na_3SbS_3 → 4 Na_3SbS_3 (-0.2034 eV)
	Co	4 Na_3SbS_3 + 8.083 Co → 0.75 Co_9S_8 + 1.333 $CoSb_3$ + 6 Na_2S (-0.1089 eV) 4 Na_3SbS_3 → 4 Na_3SbS_3 (-0.2358 eV)
	Ni	4 Na_3SbS_3 + 13 Ni → 3 Ni_3S_2 + 4 NiSb + 6 Na_2S (-0.0374 eV) 4 Na_3SbS_3 → 4 Na_3SbS_3 (-0.1900 eV)
$NaSbS_2$	V	2 $NaSbS_2$ + 1.667 V → 0.6667 Na_3VS_4 + 0.3333 V_3S_4 + 2 Sb (-1.0179 eV) 2 $NaSbS_2$ → 2 $NaSbS_2$ (-1.4963 eV)
	Cr	2 $NaSbS_2$ + 2 Cr → 2 $NaCrS_2$ + 2 Sb (0 eV)

		2 $NaSbS_2$ → 2 $NaSbS_2$ (-1.0402 eV)
	Mn	2 $NaSbS_2$ + 2 Mn → 0.6667 Na_3SbS_3 + 2 MnS + 1.333 Sb (-0.4704 eV) 2 $NaSbS_2$ → 2 $NaSbS_2$ (-0.5422 eV)
	Fe	2 $NaSbS_2$ + 2 Fe → 0.6667 Na_3SbS_3 + 0.6667 FeS + 1.333 FeSbS (-0.2034 eV) 2 $NaSbS_2$ → 2 $NaSbS_2$ (-0.3771 eV)
	Co	2 $NaSbS_2$ + 2.694 Co → 0.25 Co_9S_8 + 0.6667 Na_3SbS_3 + 0.4444 $CoSb_3$ (-0.2358 eV) 2 $NaSbS_2$ → 2 $NaSbS_2$ (-0.3648 eV)
	Ni	2 $NaSbS_2$ + 4.333 Ni → 0.6667 Na_3SbS_3 + Ni_3S_2 + 1.333 NiSb (-0.1900 eV) 2 $NaSbS_2$ → 2 $NaSbS_2$ (-0.2702 eV)
Na_2S	V	2 Na_2S → 2 Na_2S (0 eV)
	Cr	2 Na_2S → 2 Na_2S (0 eV)
	Mn	2 Na_2S → 2 Na_2S (0 eV)
	Fe	2 Na_2S → 2 Na_2S (0 eV)
	Co	2 Na_2S → 2 Na_2S (0 eV)
	Ni	2 Na_2S → 2 Na_2S (0 eV)

Table S7. Detailed chemical reactions and critical chemical potentials from grand potential phase diagram analysis for open X species (X = {O, Sb, S}) for different layered-type Na[TM]O_2 (TM = {V, Cr, Mn, Fe, Co, Ni}) cathode compounds. Note: $\mu_O = 0$, $\mu_{Sb} = 0$ and $\mu_S = 0$ are referenced to the chemical potentials of 1/2O_2 gas (μ_O^0 = -4.9355 eV), Sb metal (μ_{Sb}^0 = -4.1278 eV), and S solid (μ_S^0 = -4.1279 eV), respectively.

Compound	**Open X element**	**Critical reactions (μ_X relative to μ_X^0)**
$NaVO_2$ (@full sodiation)	O	$NaVO_2$ → $NaVO_2$ (-3.0210 eV) $NaVO_2$ → V + Na + O_2 (-4.6840 eV)
	Sb	$NaVO_2$ → $NaVO_2$ (0 eV)
	S	$NaVO_2$ → $NaVO_2$ (-1.1630 eV)
VO_2 (@full desodiation)	O	2 VO_2 → 2 VO_2 (-1.3608 eV) 2 VO_2 → 0.6667 V_3O_5 + 0.3333 O_2 (-2.1908 eV)
	Sb	2 VO_2 → 2 VO_2 (-1.5958 eV)
	S	2 VO_2 → 2 VO_2 (-1.7449 eV)
$NaCrO_2$ (@full sodiation)	O	$NaCrO_2$ → $NaCrO_2$ (-1.2456 eV) $NaCrO_2$ → Cr + Na + O_2 (-4.5194 eV)
	Sb	$NaCrO_2$ → $NaCrO_2$ (0 eV)
	S	$NaCrO_2$ → $NaCrO_2$ (-1.0065 eV)
CrO_2 (@full desodiation)	O	2 CrO_2 → 2 CrO_2 (-0.2880 eV) 2 CrO_2 → Cr_2O_3 + 0.5 O_2 (-0.5836 eV)
	Sb	2 CrO_2 → 2 CrO_2 (-5.4118 eV)
	S	2 CrO_2 → 2 CrO_2 (-6.4591 eV)
$NaMnO_2$ (@full sodiation)	O	2 $NaMnO_2$ → 2 $NaMnO_2$ (-1.1808 eV) 2 $NaMnO_2$ → $Na_2Mn_2O_3$ + 0.5 O_2 (-3.7410 eV)
	Sb	2 $NaMnO_2$ → 2 $NaMnO_2$ (-0.7291 eV)
	S	2 $NaMnO_2$ → 2 $NaMnO_2$ (-1.8060 eV)
MnO_2 (@full desodiation)	O	4 MnO_2 → 4 MnO_2 (0 eV) 4 MnO_2 → 2 Mn_2O_3 + O_2 (-0.7220 eV)
	Sb	4 MnO_2 → 4 MnO_2 (-4.8282 eV)
	S	4 MnO_2 → 4 MnO_2 (-6.1673 eV)
$NaFeO_2$ (@full sodiation)	O	2 $NaFeO_2$ → 2 $NaFeO_2$ (0 eV) 2 $NaFeO_2$ → 0.6667 Na_3FeO_3 + 1.333 Fe + O_2 (-3.6000 eV)
	Sb	2 $NaFeO_2$ → 2 $NaFeO_2$ (0 eV)
	S	2 $NaFeO_2$ → 2 $NaFeO_2$ (-1.3806 eV)

FeO_2 (@full desodiation)	O	2 FeO_2 → 2 Fe + 2 O_2 (-3.3572 eV)
	Sb	2 FeO_2 → Fe_2O_3 + 0.5 O_2 (-6.8397 eV)
	S	2 FeO_2 → Fe_2O_3 + 0.5 O_2 (-8.3005 eV)
$NaCoO_2$ (@full sodiation)	O	2 $NaCoO_2$ → 2 $NaCoO_2$ (-0.6634 eV) 2 $NaCoO_2$ → 1.333 CoO + 0.6667 Na_3CoO_3 + 0.3333 O_2 (-2.5832 eV)
	Sb	2 $NaCoO_2$ → 2 $NaCoO_2$ (-2.7485 eV)
	S	2 $NaCoO_2$ → 2 $NaCoO_2$ (-3.6036 eV)
CoO_2 (@full desodiation)	O	4 CoO_2 → 4 CoO_2 (0 eV) 4 CoO_2 → 1.333 Co_3O_4 + 1.333 O_2 (-0.1600 eV)
	Sb	4 CoO_2 → 4 CoO_2 (-6.2564 eV)
	S	4 CoO_2 → 4 CoO_2 (-7.5514 eV)
$NaNiO_2$ (@full sodiation)	O	2 $NaNiO_2$ → 2 $NaNiO_2$ (-0.0040 eV) 2 $NaNiO_2$ → 0.4 Na_5NiO_4 + 1.6 NiO + 0.4 O_2 (-1.5018 eV)
	Sb	2 $NaNiO_2$ → 2 $NaNiO_2$ (-6.1942 eV)
	S	2 $NaNiO_2$ → 2 $NaNiO_2$ (-7.3372 eV)
NiO_2 (@full desodiation)	O	NiO_2 → Ni + O_2 (-3.7290 eV)
	Sb	NiO_2 → 0.3333 Ni_3O_4 + 0.3333 O_2 (-6.8918 eV)
	S	NiO_2 → 0.3333 Ni_3O_4 + 0.3333 O_2 (-8.4912 eV)

Table S8. Detailed chemical reactions and critical chemical potentials from grand potential phase diagram analysis for open X species (X = {O, Sb, S}) for different electrolyte/electrolyte-related compounds. Note: $\mu_O = 0$, $\mu_{Sb} = 0$ and $\mu_S = 0$ are referenced to the chemical potentials of $1/2O_2$ gas (μ_O^0 = -4.9355 eV), Sb metal (μ_{Sb}^0 = -4.1278 eV), and S solid (μ_S^0 = -4.1279 eV), respectively.

Compound	**Open X element**	**Critical reactions (μ_X relative to μ_X^0)**
Na_3SbS_4	O	2 Na_3SbS_4 → 2 Na_3SbS_4 (-3.0102 eV)
	Sb	2 Na_3SbS_4 → 2 Na_3SbS_4 (-1.0216 eV) 2 Na_3SbS_4 → 3 Na_2S + 5 S + 2 Sb (-2.9677 eV)
	S	2 Na_3SbS_4 → 2 Na_3SbS_4 (0 eV) 2 Na_3SbS_4 → 2 Na_3SbS_3 + 2 S (-0.6742 eV)
Na_3SbS_3	O	4 Na_3SbS_3 → 4 Na_3SbS_3 (-3.0512 eV)
	Sb	4 Na_3SbS_3 → 4 Na_3SbS_3 (0 eV) 4 Na_3SbS_3 → 2.4 Na_3SbS_4 + 2.4 Na_2S + 1.6 Sb (-1.2822 eV)
	S	4 Na_3SbS_3 → 4 Na_3SbS_3 (-0.6742 eV) 4 Na_3SbS_3 → 6 Na_2S + 4 Sb + 6 S (-1.5290 eV)
$NaSbS_2$	O	2 $NaSbS_2$ → 2 $NaSbS_2$ (-2.8492 eV)
	Sb	2 $NaSbS_2$ → 2 $NaSbS_2$ (0 eV) 2 $NaSbS_2$ → 0.6667 Na_3SbS_4 + 1.333 S + 1.333 Sb (-1.6958 eV)
	S	2 $NaSbS_2$ → 2 $NaSbS_2$ (0 eV) 2 $NaSbS_2$ → 0.6667 $NaSbS_2$ + 1.333 Sb + 2 S (-1.3553 eV)
Na_2S	O	2 Na_2S → 2 Na_2S (-3.0946 eV)
	Sb	2 Na_2S → 2 Na_2S (0 eV)
	S	2 Na_2S → 2 Na_2S (0 eV) 2 Na_2S → 4 Na + 2 S (-3.8831 eV)

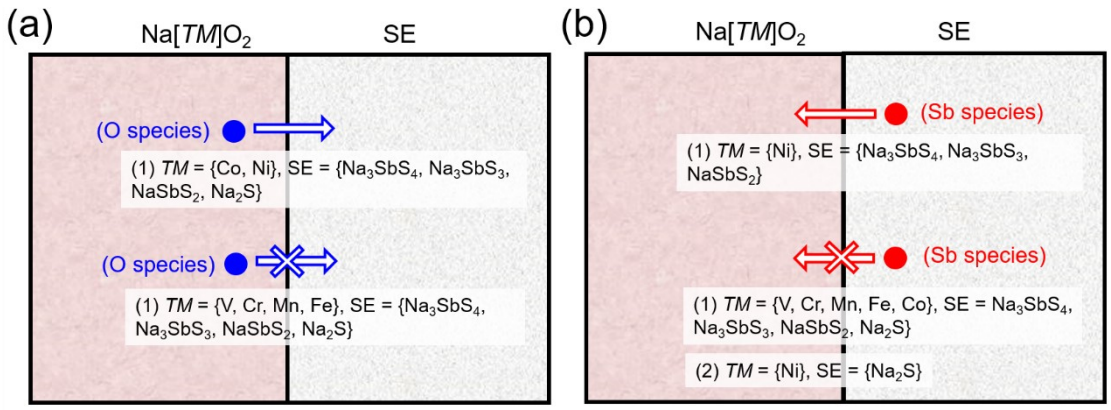

Figure S5. a-b) Schematic illustration summary for X = {O, Sb, S} species tendency to migrate across the Na[*TM*]O_2-SE interface (SE: solid electrolyte).

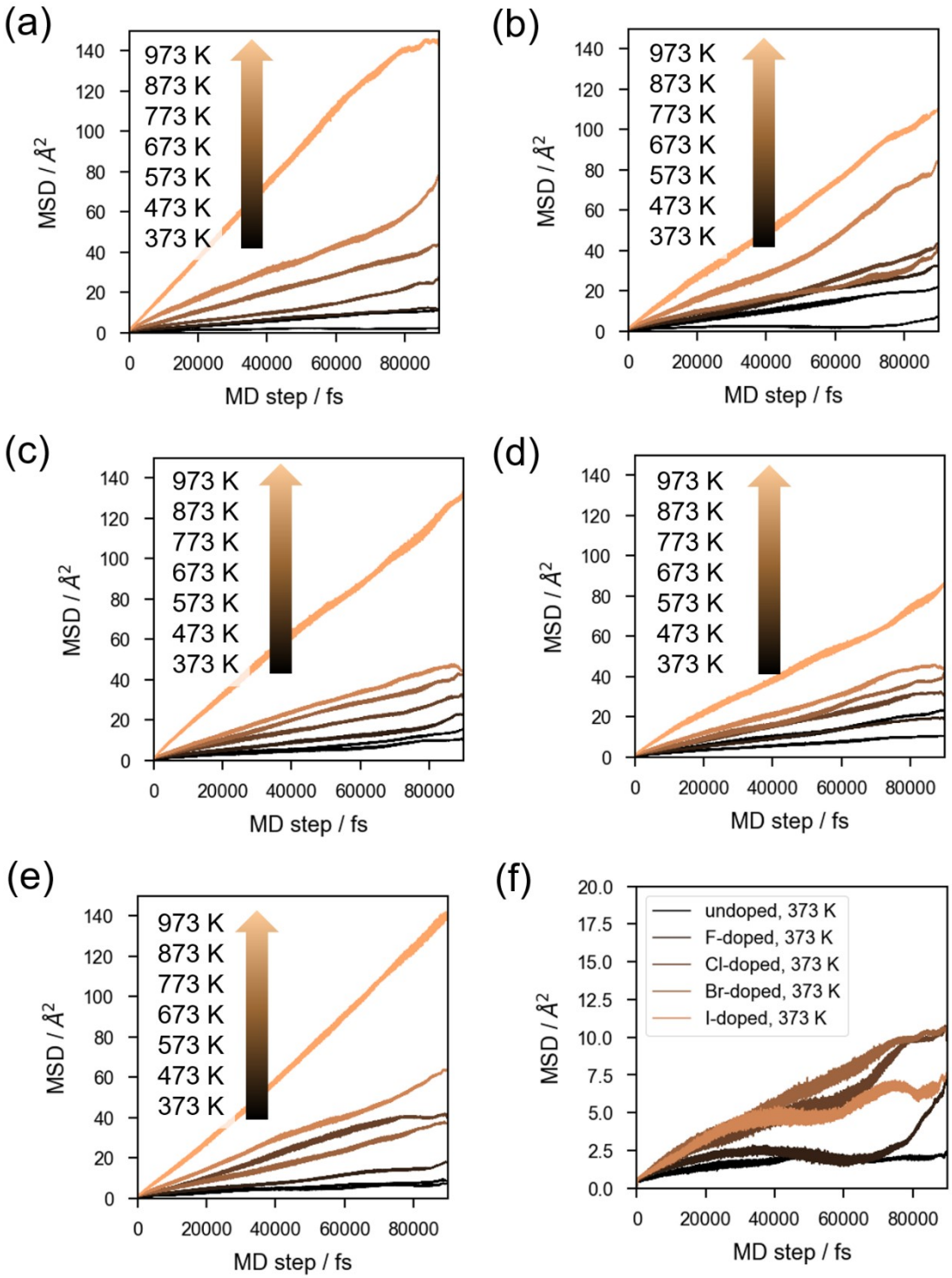

Figure S6. Mean square displacement (MSD) plots derived from DFT-MD calculations: a) 1-vacancy undoped (1v-u), b) 2-vacancy F-doped (2v-F) , c) 2-vacancy Cl-doped (2v-Cl) , d) 2-vacancy Br-doped (2v-Br), e) 2-vacancy I-doped (2v-I) model, and f) highlighted MSD plots at 373-K for a-e.

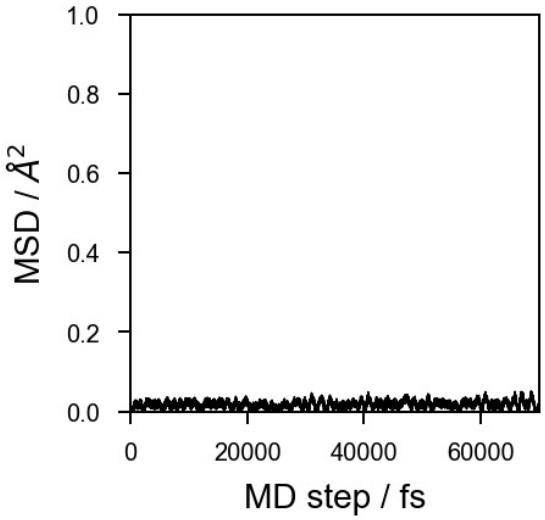

Figure S7. Li-atom mean square displacement (MSD) plot of c-NSS from DFT-MD calculation under NVT ensemble condition at 473 K.

Diffusion barrier calculation

Nudged elastic band (NEB) supercell (2 x 2 x 2) method was used to estimate ion diffusion barrier values.[59] For the Na local pathway, 7 intermediate images were interpolated linearly between fully optimized initial and final structure coordinate data. Energy barriers were then obtained in the dilute vacancy limit (or one vacancy/supercell) with cell edges of at least 14 Å.

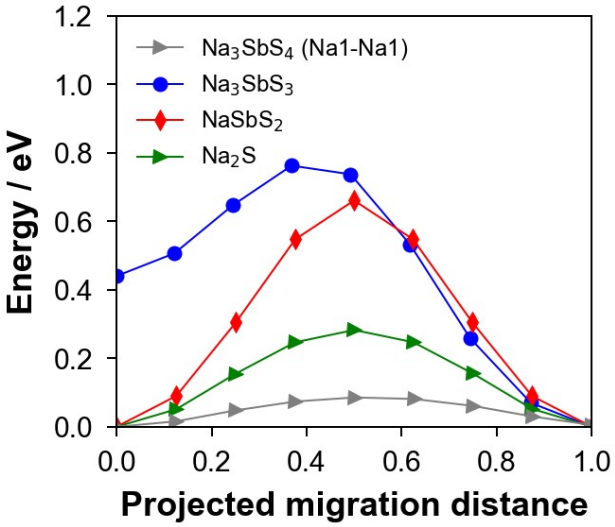

Figure S8. DFT-NEB Na ion migration energy comparison for Na1-Na1 pathway for Na_3SbS_4 and related compounds.

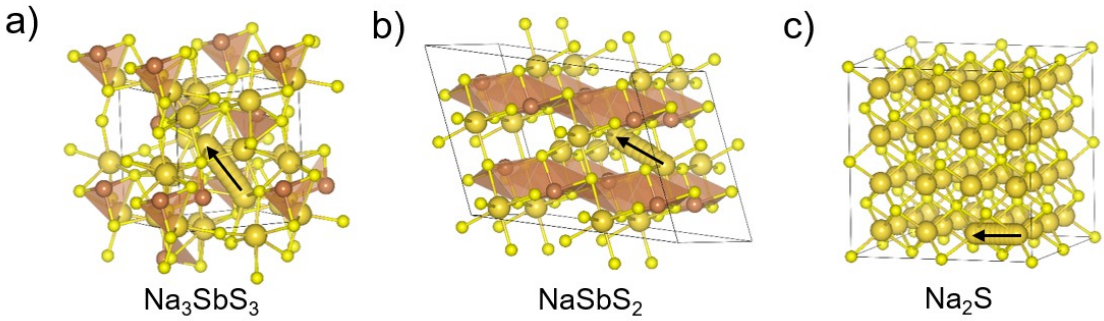

Figure S9. Visualization of local Na pathways calculated by DFT-NEB for SE-related compounds: a) Na_3SbS_3, b) $NaSbS_2$, c) Na_2S.

Table S9. Summary of DFT-predicted decomposition reactions related to voltage stability window for Na with Cl-doped Na_3SbS_4.

Voltage (V vs. Na/Na^+)	**Decomposition reaction**
0	$2Na_{23}Sb_8S_{31}Cl + 128Na \rightarrow 16Na_3Sb + 62Na_2S + 2NaCl$
0.53	$2Na_{23}Sb_8S_{31}Cl + 96Na \rightarrow 16NaSb + 62Na_2S + 2NaCl$
0.65	$2Na_{23}Sb_8S_{31}Cl + 80Na \rightarrow 62Na_2S + 2NaCl + 16Sb$
1.17	$2Na_{23}Sb_8S_{31}Cl + 32Na \rightarrow 16Na_3SbS_3 + 14Na_2S + 2NaCl$
1.54	$2Na_{23}Sb_8S_{31}Cl + 18Na \rightarrow 14NaS + 16Na_3SbS_3 + 2NaCl$
1.56	$2Na_{23}Sb_8S_{31}Cl + 11Na \rightarrow 7NaS_2 + 16Na_3SbS_3 + 2NaCl$
1.65	$2Na_{23}Sb_8S_{31}Cl \rightarrow 15NaS_2 + 16NaSbS_2 + 2NaCl + 13Na$
1.82	$2Na_{23}Sb_8S_{31}Cl \rightarrow 16NaSbS_2 + 6Na_2S_5 + 2NaCl + 16Na$
2.18	$2Na_{23}Sb_8S_{31}Cl \rightarrow 7.6Na_2S_5 + 8Sb_2S_3 + 2NaCl + 28.8Na$
2.22	$2Na_{23}Sb_8S_{31}Cl \rightarrow 6.733Na_2S_5 + 7.667Sb_2S_3 + 0.6667SbS_8Cl_3 + 32.53Na$
3.38	$2Na_{23}Sb_8S_{31}Cl \rightarrow 7.667Sb_2S_3 + 0.6667SbS_8Cl_3 + 33.67S + 46Na$